

A hybrid approach to quantifying rockfall risk with limited knowledge: a case study in Aosta Valley

Original

A hybrid approach to quantifying rockfall risk with limited knowledge: a case study in Aosta Valley / Marchelli, M., De Biagi, V., Paganone, M., Bertolo, D.. - In: BULLETIN OF ENGINEERING GEOLOGY AND THE ENVIRONMENT. - ISSN 1435-9529. - 84:11(2025), pp. 1-21. [10.1007/s10064-025-04513-7]

Availability:

This version is available at: 11583/3003826.6 since: 2025-10-09T16:03:03Z

Publisher:

Springer Nature

Published

DOI:10.1007/s10064-025-04513-7

Terms of use:

This article is made available under terms and conditions as specified in the corresponding bibliographic description in the repository

Publisher copyright

(Article begins on next page)



A hybrid approach to quantifying rockfall risk with limited knowledge: a case study in Aosta Valley

Maddalena Marchelli¹ · Valerio De Biagi² · Marco Paganone³ · Davide Bertolo³

Received: 8 October 2024 / Accepted: 18 September 2025
© The Author(s) 2025

Abstract

The quantification of rockfall risk along an infrastructure is a fundamental achievement for an appropriate management of mountain roads and it consists of various steps: from the identification of the sources and sizes of the potential unstable blocks, to the trajectory analysis and, finally, the quantification of the effects on the elements at risk. The degree of knowledge of the slope and the previous rockfall events provides a solid base for the calculation and a precise risk quantification can be obtained for areas of limited extent. On the contrary, when moving to areas of large extent the previous steps cannot be completely achieved and the risk has to be computed by considering the effects of the limited knowledge. To this aim, the paper details a procedure to include the effect of uncertainties into the quantification of the societal risk along a road. The proposed method is a hybrid quantitative approach that integrates elements of likelihood-based, fuzzy, and Bayesian methodologies. It is specifically designed for rockfall risk assessments over extensive areas under conditions of limited data availability. To address epistemic uncertainty, the method primarily involves assigning likelihoods to the frequency of blocks reaching the road, based on historical data, in order to estimate a range of potential risks and their associated probabilities. Aleatory uncertainty inherent in the phenomenon is handled using Monte Carlo probabilistic techniques. To explain the various steps in the analysis, the proposed approach is applied to a study case consisting of a 7.5 km long touristic road subjected to rockfall hazard in Aosta Valley, in the Northwestern Italian Alps, considering different possible traffic scenarios. It is shown that the method is suitable to determine the risk when the knowledge of the area is limited.

Keywords Rockfall · Quantitative analysis · Road · Hazard · Risk assessment · Hybrid methods · Uncertainties

Introduction

Rockfall risk analysis is an essential aspect in the management of mountainous regions, where geohazards pose significant threats to infrastructure, human life, and economic activities (Hungar et al. 1999). Driven by the scientific advancements (Morgenstern 2018; Fell et al. 2005; Corominas et al. 2014; Macciotta et al. 2017), quantitative risk assessment (QRA) techniques have become increasingly adopted by Public Authorities over the past decade for decision-making in landslide-prone areas (Marchelli et al. 2022a). The ability to compare risk levels against defined thresholds enables more cost-effective management strategies.

Research on risk quantification encompasses all aspects of the rockfall phenomenon, from the identification of unstable areas and block detachment to their interaction with urbanised environments (Scavia et al. 2020). As with any complex phenomenon, the quality of input data

✉ Maddalena Marchelli
maddalena.marchelli@polito.it

Valerio De Biagi
valerio.debiagi@polito.it

Marco Paganone
m.paganone@regione.vda.it

Davide Bertolo
d.bertolo@regione.vda.it

¹ Department of Environment, Land and Infrastructure Engineering, Politecnico di Torino, Corso Duca degli Abruzzi, 24, 10129 Torino, Italy

² Department of Structural, Geotechnical and Building Engineering, Politecnico di Torino, Corso Duca degli Abruzzi, 24, 10129 Torino, Italy

³ Geological Office, Regione Autonoma Valle d'Aosta, Via Promis, 2, 11100 Aosta, Italy

significantly influences the reliability of outputs. Accurate predictions regarding source zones and the evolution of rockfall events require high-resolution topographic data, as well as detailed geological, geomorphological, meteorological, and lithological information, including vegetation cover and land use (Wei et al. 2014; Lan et al. 2010; Kanno et al. 2023). Despite progress in modelling and assessment techniques, uncertainty remains a pervasive challenge in predicting and mitigating rockfall hazards. These uncertainties stem from various sources: the occurrence and size of released blocks, their dynamics along the slope (including fragmentation (Marchelli et al. 2025)), and their impact on exposed elements.

For instance, the quantification of release probability remains debated, as it is influenced by numerous poorly understood variables (D'Amato et al. 2016; Moos et al. 2022). Consequently, observational techniques, e.g. periodic surveys (Budetta et al. 2016; Matasci et al. 2018; Strunden et al. 2015) or continuous monitoring (Zimmer and Sitar 2015; Feng et al. 2021), are adopted to estimate event frequency. However, these methods typically capture only recent activity. Historical inventories provide valuable long-term and large-scale records of rockfall activity (Dussauge et al. 2003; Hungr et al. 1999), though they are often biased due to unobserved events (Volkwein et al. 2011). De Biagi et al. (2017) addressed this issue by introducing a threshold volume in observations. While vegetation damage can indicate past events (Trappmann et al. 2013; Favillier et al. 2017), such evidence is generally limited to major occurrences. Recently, Farvacque et al. (2021) integrated dendrochronological data and deposit observations from rockfall barriers with 3D modelling to estimate the frequency of different block volumes. Block volume is strongly influenced by discontinuity set characteristics. Umili et al. (2023) proposed a new formula, based on Palmström's expression, to account for aleatory variability in real rock faces. Volume and shape are key inputs for propagation analysis, which is further affected by rock–soil interactions (Agliardi and Crosta 2003; Crosta and Agliardi 2004). Li and Lan (2015) reviewed the uncertainties in trajectory modelling, highlighting their dependence on model selection, assumptions, and input accuracy.

Risk quantification, resulting from release, propagation, and interaction, is inherently affected by these uncertainties. Addressing uncertainties is a challenge that extends well beyond the rockfall sector; disciplines such as economics and the social sciences have developed suitable approaches to incorporate both aleatory and epistemic uncertainties into risk assessment (Shortridge et al. 2017).

In rockfall framework, aleatory uncertainty, that depends on the inherent random variability of processes, is influenced by factors such as lithology, random distribution of

fractures in the rock (Wang et al. 2012, 2014a). The uncertainty in the size of the released block has generally been tackled by considering different volumes and assigning to each of them their return period according to a volume–return period law. Although there are evident difficulties in estimating the relationship in the source area (Wang et al. 2014a), the volume–frequency law can be related to a power-law (Dussauge et al. 2003; Hantz et al. 2016; Macciotta et al. 2020). Such approach has been adopted by the Authors in quantifying the reliability of a rockfall barrier (De Biagi et al. 2020; Marchelli et al. 2020a, 2021). To reduce the impact of aleatory uncertainties on the propagation, say on the trajectory analysis, a probabilistic approach is thus requested and a large number of throws is necessary. In particular, a Monte Carlo approach is widely used in trajectory analyses and hazard assessment to address aleatory uncertainty. By repeatedly sampling from probability distributions assigned to the input variables, Monte Carlo methods allow for the estimation of the likelihood and range of possible outcomes, such as run-out distances or impact energies (Dorren 2003; Macciotta et al. 2015). It is worth mentioning that despite widely adopted to model aleatory uncertainty, Monte Carlo approach has notable limitations, as it requires high-quality input data, and poor-quality data can lead to misleading results (Dorren 2003). Moreover, many rockfall trajectory models simplify physics (e.g., constant restitution coefficients), reducing realism when amplified through stochastic sampling (Chen et al. 2013).

Epistemic uncertainty in rockfall modelling arises from limited knowledge about key factors such as source location, event frequency, propagation methods, and parameter selection. This uncertainty is compounded by the difficulty in directly measuring essential parameters and the impracticality of full-scale experiments. As a result, significant gaps remain in understanding material behaviour, block geometry, slope topography, and block–slope interaction mechanics. Thus, both data-related and model-related uncertainties fall under the category of epistemic uncertainty (Rangava-jhala et al. 2012). For instance, Mineo (2020) compared various risk analysis techniques, highlighting differences in the level of detail, the treatment of uncertainty, and the assumptions required. To account for it, various suggestions are possible, also in other disciplines, including computer science and safety engineering. As an example, dealing with QRA for a generic hazardous event and a generic risk, Aven (2008) has proposed to include semi-quantitative uncertainty factors as an additional component of the risk analysis with the specific purpose to state the knowledge that supports the result. Lempert et al. (2006) have repeated the same analysis several times with slightly different initial conditions to assess the outputs and check for the effects of uncertainty. Besides traditional models, fuzzy logic approaches can be

adopted (De Ru and Eloff 1996), providing a framework for handling vagueness and imprecision in input data. In fuzzy logic, membership functions are used to express the degree of truth or confidence in qualitative or uncertain information, such as the likelihood of a slope being unstable or the severity of potential impacts, rather than relying on binary or crisp values. These functions allow for a more flexible representation of expert knowledge and subjective assessments within the risk analysis process. Building on this framework, fuzzy numbers, i.e. a specific type of fuzzy set used to represent uncertain numerical quantities, have been applied to model epistemic uncertainties in rockfall simulations. For instance, Turrin et al. (2009) proposed the use of fuzzy numbers to represent uncertainties in material properties and boulder geometry. This approach enables the quantification and propagation of uncertainty through fuzzy transformation methods, which can be used to derive ranges for key parameters such as coefficients of restitution, essential for simulating block-slope interaction behaviour. Nevertheless, while fuzzy logic models offer a flexible framework for incorporating expert judgment and handling imprecise, scarce or qualitative data, they also present notable limitations, including the subjectivity in defining membership functions and rules, which can affect reproducibility. Additionally, fuzzy models lack a probabilistic foundation, making it difficult to quantify risk in terms of likelihood or to integrate them with physically based models for dynamic processes like block trajectories (Shang and Kossen 2013). A probabilistic framework that allows for the explicit incorporation and representation of epistemic uncertainties in risk analysis relies in Bayesian networks, a model that represents a set of variables and their conditional dependencies, and the associated process of Bayesian inference, which updates probabilities as new data becomes available (Fenton and Neil 2018; Kaikkonen et al. 2021). In the context of rockfall hazard assessment, Bayesian inference provides thus a systematic way to update prior beliefs on many input parameters subject to epistemic uncertainty due to limited data or measurement challenges as new evidence becomes available, resulting in posterior distributions that reflect improved knowledge. By integrating both expert judgment and observational data, Bayesian networks allow for the dynamic refinement of probability distributions, resulting in posterior estimates that reflect improved knowledge. However, despite their advantages, the practical application of Bayesian networks in geohazard modelling presents several challenges. These include the need for substantial expert input to define the network structure and assign prior probability distributions, which can be subjective and difficult to validate in data-scarce environments (Zheng et al. 2021). Acquiring sufficient and reliable data to support inference is often problematic, especially in mountainous or

inaccessible regions where rockfall and landslide events are underreported or poorly documented (Hwang et al. 2024). Moreover, the quality of the results is highly dependent on the accuracy of the conditional probability tables and the assumptions embedded in the model. Incomplete or biased data can lead to misleading posterior distributions, reducing the robustness of the risk assessment. These limitations highlight the importance of the integration of expert knowledge with empirical data to ensure meaningful and actionable outcomes in geohazard risk analysis (Cardenas et al. 2022).

To enhance predictive accuracy and manage epistemic uncertainties, machine learning (ML) techniques, ranging from decision trees to deep learning, are increasingly being applied to rockfall hazard and risk assessment (Farmakis et al. 2022, 2025; Fanos et al. 2020; Chanut et al. 2024). For example, deep learning models can identify hidden patterns within large datasets, thereby compensating for gaps in expert knowledge and reducing epistemic uncertainty (Abaker et al. 2023). However, aleatory uncertainty remains more challenging to address, even though some studies attempt to incorporate probabilistic frameworks or ensemble modelling to partially capture this variability (Wang et al. 2014b). Despite their promise, ML-based methods face several challenges. First, the site-specific nature of rockfalls limits the generalizability of trained models. Second, the scarcity and imbalance of labelled data (e.g., relatively few rockfall events compared to non-events) can bias predictions. Third, interpretability remains a concern—particularly for deep learning models, which are often perceived as “black boxes”. This necessitates careful calibration and validation to ensure model reliability and stakeholder trust (He et al. 2024).

In situations where quantitative data are scarce or incomplete, or in large-scale assessments and operational settings where detailed simulations may be impractical due to time or data constraints, likelihood-based scoring systems are widely adopted in rockfall hazard assessment. These methods are often qualitative in nature, relying on expert judgment and field observations to assign likelihood ratings to potential rockfall events through structured checklists or rating matrices (Ferrari et al. 2016; Farmer et al. 2023; Pandey et al. 2025).

Finally, Wang et al. (2014a) have addressed both aleatory and epistemic uncertainties by assigning coefficients of variation to input variables and applying a first-order second-moment method to propagate variance. They modelled the release process using a power-law relationship between block size and frequency, offering a structured probabilistic framework. However, this approach requires well-characterised input data, which may limit its applicability in data-scarce environments. Across the key studies, Macciotta and

co-authors have progressively refined their approach to managing uncertainty in slope risk assessment. In the 2016 railway case study (Macciotta et al. 2016b), aleatory uncertainty has been addressed through Monte Carlo simulations, while epistemic uncertainty has been managed via expert judgement and bounding estimates. The 2020 Canmore highway study (Macciotta et al. 2020) has adopted a probabilistic QRA framework, incorporating multiple release scenarios (e.g., block size, frequency), sensitivity analysis, and the use of upper and lower bounds for uncertain parameters to address both types of uncertainty. Nevertheless, both studies rely on detailed site-specific data and expert calibration, making them more suitable for local-scale applications with sufficient information. In Macciotta (2023), the authors shifted the focus towards the documentation of uncertainty sources and the influence of environmental variability, particularly under climate change. While conceptually robust, this framework may be less effective for detailed design or mitigation planning without supporting data.

In the present study, we propose a hybrid quantitative method that integrates elements of likelihood-based, fuzzy, and Bayesian approaches, specifically designed for large-scale rockfall risk assessments under conditions of scarce data. This approach addresses a critical gap in current methodologies, which are often either qualitative or require extensive datasets, by enabling probabilistic reasoning and uncertainty quantification even when empirical data are limited. Our model assigns a likelihood, expressed as a probability, to the most critical source of epistemic uncertainty in rockfall risk assessment, i.e. the frequency with which a rock block impacts an element at risk. This probability is derived from historical event data but can be dynamically updated as new information becomes available, incorporating prior knowledge in a Bayesian sense. As such, the method occupies a conceptual space between fuzzy logic and Bayesian inference: it retains the interpretability and flexibility of fuzzy approaches while enabling probabilistic updating typical of Bayesian frameworks. In parallel, aleatory uncertainties are addressed through a probabilistic approach using Monte Carlo sampling techniques, with particular reference to the propagation phase of rockfall modelling, allowing for a robust estimation of impact probabilities and spatial hazard metrics. The hybrid structure of the method thus ensures comprehensive treatment of both epistemic and aleatory uncertainties, making it particularly well-suited for large-scale applications where uncertainty is high and data availability is limited.

This study originates from a specific request of the Local Authority of having a general quantification of the societal risk, i.e. probability of having fatalities, along a 7.5 km touristic road in Northwestern Italian Alps, which experienced rockfall problems in the past along almost its entire

length, to further manage the risk along the infrastructure. The information on the geological context was extremely limited: neither specific survey on the potential source zones nor geomechanical analyses were available. Given the extensive size of the study area, large-scale remote sensing is neither economically viable nor practically feasible. As a result, simplifications and assumptions regarding potential block volumes and frequencies if the events are necessary, since acquiring detailed knowledge is not possible (Scavia et al. 2020). Such level of detail, which can be achieved when the study area is limited in size, cannot be reached when moving to a large extent, as in the present study case. In this work, a specific risk assessment method based on Event Tree Analysis (ETA), developed by the Authors (Marchelli 2020; Marchelli et al. 2022a), is applied. This method incorporates the proposed hybrid approach to address uncertainties, particularly those related to the frequency of block impacts on elements at risk, which emerges as the most relevant parameter in the overall risk evaluation. The paper details the performed calculations, discusses the underlying hypotheses, and reports the results of the risk analysis.

The paper is organised as follow. First, the fundamentals of rockfall risk assessment on vehicular roads are presented (Section “[Basics of risk calculation on roads](#)”). The methodology for addressing uncertainties, along with the underlying assumptions, is introduced in Section “[Methodology](#)”. Section “[Case study](#)” is entirely dedicated to the description of the case study and the presentation of the analysis results. The effects of uncertainty are discussed, and suggestions for risk management are provided in Section “[Discussions](#)”. Finally, the conclusions (Section “[Conclusions](#)”) summarize the main steps of the analysis.

Basics of risk calculation on roads

The present section summarizes the basics concepts of quantitative risk assessment with a particular focus on an approach to quantify rockfall risk on roads, previously developed by the Authors (Marchelli 2020; Marchelli et al. 2022a). This approach constitutes the analytical framework employed in the present study, whose variables are treated using methods that account for both epistemic and aleatory uncertainties, incorporating likelihood-based reasoning and statistical analysis. Thus, the presented formulae will be recalled in the methodology. Generally speaking, the risk is determined as function of the hazard, the exposure, the vulnerability, and the value (capacity) (Corominas et al. 2014; Fell et al. 2008), and its calculation should account for the previously mentioned large uncertainties in the phenomenon (Li and Lan 2015; Beven et al. 2018). Dealing

with infrastructures, the risk quantification should be usually related to the average consequences in terms of societal risk, that gives a risk value for a whole area, no matter precisely where the harm occurs within that area, being function of the frequency of each hazard (Melzner et al. 2020; De Biagi 2017), the total number of people affected and their exposure (Jonkman et al. 2003; Muhlbauer 2004). As often required by policy-makers, the societal risk is calculated in terms of annual probability of having at least one damage (fatality), approximated to the number of damages per year. For elements at risk with non unitary exposure, e.g. moving vehicles, the Authors have proposed a method to quantify the fatal and injury-related consequences of a block reaching the road, based on an event-tree approach (ETA) (Marchelli 2020; Marchelli et al. 2022a), which is commonly used for risk assessment along transportation corridors (Bunce et al. 1997a; Mignelli et al. 2012; Mineo 2020; Macciotta et al. 2016a). In this method, the occurrence probability of a rockfall event is considered in both spatial and temporal dimensions.

The ETA approaches are rooted from the occurrence of an event, starting from which all the possible scenarios and outcomes are evaluated. Here, the element at risk is the vehicle with travellers inside. The arrival on a block on the road is the initiating event, following which two mutually exclusive scenarios can develop: the block can hit the element at risk or not. In the latter case, the block can rebound on road pavement, even damaging its surface or stop on it. Each scenario could lead to fatality or injury, according to several parameters, related to exposure (i.e. the speed and the size of the vehicle, the number of people inside) and element’s features (i.e. the ratio between the decision and the stopping sight distances, and the traffic conditions), and it is characterised by a probability. The probability of adverse outcome (say, victim) is obtained as the summation of the

probabilities of each scenario leading to a victim among the travellers.

The entire road can be divided into portions of typically 50 to 100 meters in length, which are homogeneous in terms of traffic conditions (e.g., speed, sight distance, gradient, etc.). Figure 1 reports the proposed method, which is applied for each k th portion. Given the occurrence of the initiating event, the scenarios refers to a fatal accident as outcome, and, thus, for each k th portion of road, the probability to have a fatal accident, defined PF^k is:

$$PF^k = PF_i^k + PF_s^k + PF_d^k, \tag{1}$$

where the subscripts i , s , and d refer to the case that (i) a moving vehicle is hit by the falling block, or (s) a moving vehicle impacts on the block stopped on the road, or (d) a moving vehicle skids for damages on the road caused by the rebounding of the block on it. For simplicity of notation, the equations that follow do not explicitly recall the superscript k th indicating the portion of road. The occurrence of the first scenario, i.e. the block hits the vehicle, requires the contemporaneity in time and in space of the falling block and the moving vehicle which is expressed by the temporal-spatial probability $P_{(S:T)_i}$:

$$P_{(S:T)_i} = P_{(T:V)_i} P_{(S:V)_i}, \tag{2}$$

being $P_{(T:V)_i}$ and $P_{(S:V)_i}$ the temporal and spatial probabilities, respectively. As detailed in Marchelli et al. (2022a), these probabilities can be computed as the product of the probability in time and space that a single vehicle is hit throughout the year, multiplied by the hourly traffic and the annual number of hours for which this traffic condition is valid, resulting that $P_{(S:T)_i}$ is function of the average speed and the size of the vehicle. The probability that the impact

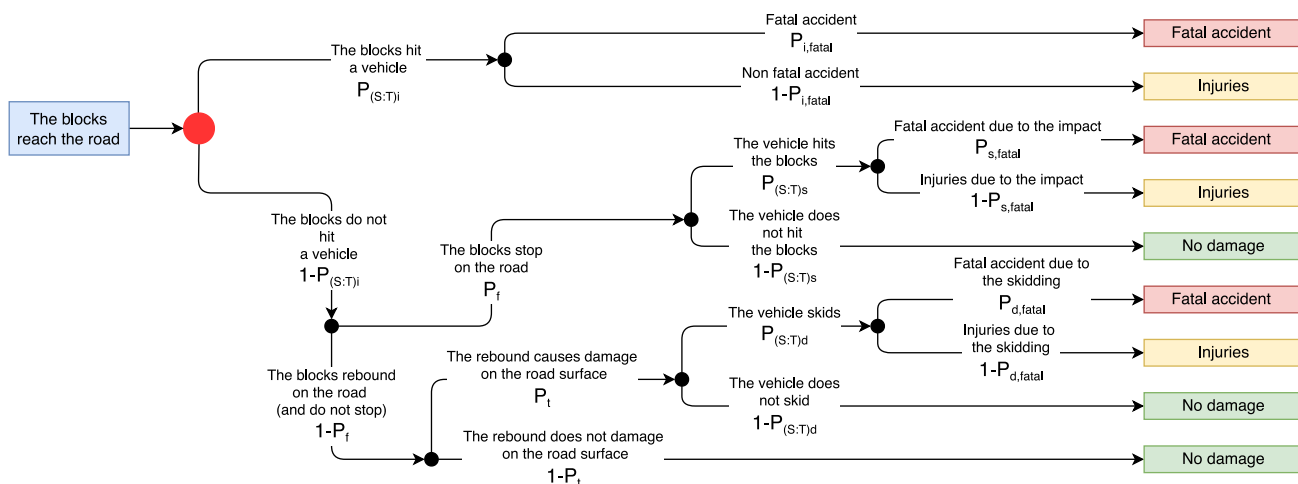


Fig. 1 Proposed method for risk assessment for people driving in a road subjected to rockfall, modified after Marchelli et al. (2022a)

leads to a fatality, $P_{i,fatal}$, depends also on the number of travellers. If resting conditions apply, e.g. in case of a parking, the stop duration must be considered in the evaluation of $P_{(T:V)_i}$. The same procedure is adopted for the other two scenarios with possible fatalities. The probability of blocks stopped on the road P_f or rebounding $(1 - P_f)$ can be computed through trajectory analyses, while the probability of damages on the road P_t derives on statistics of past observed events. The temporal spatial probability that a vehicle impacts against a stopped block is function of the decision sight distance and the speed of the vehicle. Considering notations reported in Fig. 1, the probabilities $P_{s,fatal}$ and $P_{d,fatal}$ can be computed from the annual statistics of fatal accident for similar type of road and causes. It results:

$$PF_i = P_{(S:T)_i} P_{i,fatal}, \tag{3}$$

$$PF_s = [1 - P_{(S:T)_i}] P_f P_{(S:T)_d} P_{s,fatal}, \tag{4}$$

and

$$PF_d = [1 - P_{(S:T)_i}] (1 - P_f) P_t P_{(S:T)_d} P_{d,fatal}. \tag{5}$$

Inserting Eqs. (3), (4) and (5) in Eq. (1), the probability of having a fatality in the k th portion is obtained, provided the occurrence of an event.

In such situations in which the hazard is diffused along the road, the information on past events is typically related only to the phenomena which have reached the road. The recorded data can be binned in the various parts of the track. The length of each part depends on the surrounding environment and its bounds are determined based on the analysis of the rock faces and slopes. Critical spots along the path, i.e. overhanging cliffs of limited length that often release rock blocks, are considered as specific sections. Through propagation analysis, the method also allows for the evaluation of the spatial probabilities associated with different blocks reaching the road, referred to as reaching probability. Moreover, varying traffic conditions may occur along the same road segment. To address these complexities, the road is discretized into (i) sections, (ii) portions, and (iii) sub-portions. As illustrated in Fig. 2, the entire stretch from A to D is divided into sections, each characterized by similar rockfall conditions, such as the same source area and/or comparable geomechanical properties of the slope face, resulting in a similar frequency

of blocks on the road. Each section is further divided into portions, which are homogeneous in terms of traffic conditions. Each portion is then subdivided into sub-portions, each defined by a uniform reaching probability.

Thanks to the properties of ETA and the modularity of the method, the risk can be computed for each portion and then aggregated across sections and, ultimately, along the entire road.

It is worth mentioning that the exposure model adopted in this study is designed to be modular and adaptable. While a simplified representation is used for general applicability, the model can incorporate real-world traffic variability, such as peak-hour traffic, seasonal closures, or time-dependent flow rates. Risk calculations can be performed for sub-annual intervals with consistent traffic conditions, and the resulting probabilities can be summed to estimate the total annual risk. This approach maintains the integrity of the event-tree framework while allowing for different traffic conditions. It should be noted, however, that the current model does not account for secondary vehicle incidents, such as collisions or skidding caused by evasive maneuvers during a rockfall event.

Applying all these concept, in the framework of a diffused hazard, named $N_{B,p}$ the annual frequency of events recorded in the p th section, the estimated annual frequency on the k th portion of the p th section is computed according to the reach probabilities on the path obtained from the rockfall trajectory analyses, resulting in:

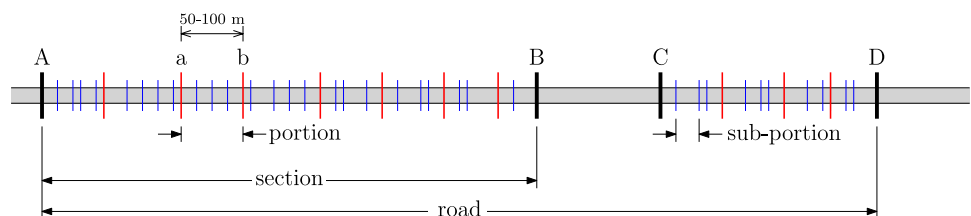
$$N_{B,k} = \frac{\Omega_k}{\sum_{j=1}^n \Omega_k} N_{B,p}, \tag{6}$$

where Ω_k derives from the weighted sum of the reach probabilities $P_{(S:B)}$ and the lengths of the r sub-portions constituting the k th portion, i.e.:

$$\Omega_k = \sum_{o=1}^r P_{(S:B)}^o \ell_o. \tag{7}$$

The summation of Eq. (6) is extended thus to the total number (n) of portions in the section. It is worth noting that the redistribution of the frequencies on the portions necessarily depends on the propagation analyses, and the choices behind their evaluation, i.e. the release zones, the block-soil interaction.

Fig. 2 Sketch of a road with its discretization. Sections are marked with thick black lines, portions with red lines, and sub-portions with blue lines



The result of Eq. (6) can be used to map for each portion of the road the probability that at least a block arrives during a τ years, namely $P_{(S:T)k}(\tau)$. Considering the rockfall occurrence process as a Poisson point process (McClung 1999; Hantz et al. 2003; Straub and Schubert 2008; Al-Shaar et al. 2024), it results:

$$P_{(S:T)k}(\tau) = 1 - \exp(-N_{B,k}\tau). \tag{8}$$

If $\tau = 1$, Equation. (8) provides the annual probability that the k th portion of road is affected by at least one rockfall event. The hypothesis that rockfall occurrences on the road follow a Poisson point process is supported, as the considered frequency pertains only to blocks that have reached the road. In this framework, if multiple blocks reach the element at risk during a single rockfall event, the event is still treated as a single occurrence. According to the definitions provided by Hantz et al. (2021), this type of occurrence can be referred to as the “event passage frequency” on the road, which relates specifically to the occurrence of a rockfall event. If the frequency of rockfalls on the section is low, the probability computed with Eq. (8) provides the probability of having a single rockfall event in the year on the road portion, and the annual probability of having a fatality, i.e. the risk, on the p th section can be computed as:

$$R_p = \sum_{k=1}^n \left\{ [1 - \exp(-N_{B,k})] PF^k \right\}, \tag{9}$$

where the summation extends to all the n portions constituting the p th section. The risk on the entire road is computed as the sum of the values for each section.

Equation (9) underestimates the real risk if the hypothesis of a low events’ frequency on the section does not hold. Hence, a more general approach based on Binomial distribution is considered. The annual probability of having at least one victim, that is the risk, on the p th section is provided by:

$$R_p = \sum_{k=1}^n \left[1 - \left(1 - PF^k \right)^{N_{B,k}} \right], \tag{10}$$

being the term in square brackets the risk in each portion.

Methodology

The variables involved in the previously described approach for quantifying the societal risk along a road are treated to address both aleatory and, more importantly, epistemic

uncertainties. To this end, a hybrid quantitative methodology is developed, tailored for large-scale rockfall risk assessments in data-scarce environments. This approach combines elements of likelihood-based reasoning, fuzzy logic, and Bayesian inference to effectively capture epistemic uncertainty. Concurrently, aleatory uncertainty is managed through a probabilistic framework employing Monte Carlo simulations, particularly during the rockfall propagation phase, enabling robust estimation of impact probabilities and spatial hazard indicators. In the following the complete QRA method is presented, recalling all the steps of the risk assessment.

First, the source areas were defined based on the geological information available, with particular emphasis on previous documented events and the (eventual) studies on the slopes insisting on the road. Given the nature of the analysis, which envisages an risk integrate along the entire road, the detailed geomechanical analysis consisting in the identification of the discontinuity sets, the release mechanisms, and the in-situ block sizes distribution were performed for a limited number of cliffs selected as representative of the whole conditions. The identified source areas were reported in a GIS environment. Then, the whole road was divided into sections, according to the definition previously stated, which are characterised by similar geomechanical conditions of the face and geomorphology of the slope, resulting in a homogeneous potential release frequency. The second step consisted in the definition of the blocks arrival frequencies and the related uncertainties. The frequency of occurrence of rockfall blocks reaching, for example, the p th section, $N_{B,p}$, was estimated based on the knowledge of previous documented events and the information obtained from non-documented events such as: damages to road pavement, blocks intercepted by the vegetation in the surroundings of the road, blocks intercepted by protective structures (net fences), etc. As the operation of calculating the frequency of rockfalls is affected by epistemic uncertainty, the Authors considered two additional frequencies of occurrence for each section, i.e. $N_{B,p}^-$ and $N_{B,p}^+$. The former was obtained dividing $N_{B,p}$ times 1.5 to consider that the process is less frequent than expected, the latter multiplying the figure times 1.5 to consider that the process is more frequent than expected. A probability (like a prior probability) is associated to the three frequencies to measure the likelihood of the assumption. In other words, $\mathcal{L}_{B,p}$ is the likelihood associated to $N_{B,p}$, i.e. the probability that the annual frequency of occurrence in the p th section is $N_{B,p}$. The sum $\mathcal{L}_{B,p}^- + \mathcal{L}_{B,p}^+$, i.e. the sum of the likelihoods associated to $N_{B,p}^-$ and $N_{B,p}^+$, is the uncertainty in the estimation of the frequency. The sum of the three like likelihoods is one:

$$\mathcal{L}_{B,p}^- + \mathcal{L}_{B,p} + \mathcal{L}_{B,p}^+ = 1. \quad (11)$$

Based on the various soil types, back-analysis of previous events, and available literature on similar environments, the propagation analyses were conducted within a probabilistic framework using Monte Carlo sampling techniques. This allowed for the determination of reaching probabilities and the subdivision of the area into distinct sub-portions. Finally, realistic traffic scenarios were defined and the calculations of the risk according to the formulae presented in Section “Basics of risk calculation on roads” were performed. In the present case, the considered elements at risk are people driving on a road. In this context, due to high velocities involved in a rockfall event (up to 30 m/s) and to the kinetic energies of the possible impacting blocks, it was assumed that any block of any size could cause damage. This assumption is supported by multiple studies indicating that even small blocks can lead to severe consequences. Hoek and Karakas (2008) have reported that rockfalls have caused numerous fatalities on mountain highways, with small blocks capable of producing deadly impacts due to high velocities and slope geometries, such as ski-jump effects. Similarly, Rwozi (2010) has highlighted that small blocks can penetrate windshields or destabilize vehicles, particularly at highway speeds. Mavrouli and Corominas (2018) and Maheshwari et al. (2023) have further emphasized that any rock with sufficient kinetic energy to damage pavement can also injure or kill vehicle occupants. These findings are reinforced by vehicle safety data from the National Highway Traffic Safety Administration (NHTSA), which has indicated that occupant injuries can occur at impact speeds as low as 4–5 mph (6–8 km/h) (Nama et al. 2016), especially in low-crush scenarios where energy is transferred directly to passengers.

Three different values of risk, in terms of annual probability of having at least one fatality, were obtained for each section, each of which is associated with likelihood value, based occurrence frequency adopted in the calculation. Equation (10) was arranged to include the likelihood value on the occurrence frequency:

$$R_p = \sum_{\ell=1}^3 \mathcal{L}_{B,p}^{\ell} \left\{ \sum_{k=1}^n \left[1 - \left(1 - \text{PF}^k \right)^{N_{B,k}^{\ell}} \right] \right\}. \quad (12)$$

It is worth to note that the approach holds for any number of occurrence frequencies (hence, not necessarily 3 as done by the Authors), provided that the corresponding likelihoods respect Eq. (11). Considering that the road is made of a total of s sections, 3^s combinations of the risk values were evaluated. For each combination, the risk along the entire road was computed as the sum of the single risks, and the

likelihood associated was the product of the single likelihoods. This allowed to associate a confidence value to the quantified risk, as presented in Section “Case study”.

Case study

The methodology described in Section “Methodology” is applied to a case study in Valpelline valley in Aosta Valley, Northwestern Italian Alps. Valpelline is a 33 km long valley that starts 6.5 km north of Aosta and runs NE-SW parallel to the border between Italy and Switzerland (Wallis canton). Figure 3 sketches the area and the geographical context. At about three-quarters of the length of the valley the Places Moulin dam, a 136 m high double-curvature reinforced concrete dam, is located. The dam forms an artificial lake located at 1965 m a.s.l. and 6.5 km long with a capacity of 105 Mm³ that serves as storage for precipitations and melt water from the glaciers that are present in the upper part of the valley and flow along Buthier creek. A sealed road stretching from Bionaz village to the dam and built in the Sixties (in yellow in Fig. 3) is open from April to October and closed in the winter period due to snow avalanche hazard. The accessibility of the dam during the winter season is guaranteed via helicopter. The dam site and the lake are very popular among tourists, and the parking area located close to it is the starting point for several hikes and mountain trails. The 7.5 km long road is the only route of access to the dam and the high part of Valpelline valley. In 2023, Bionaz municipality has counted more than 13k vehicles in the paying parking lots. Three types of vehicles access the road: cars (88%), coaches (2%) and motorcycles (10%) with an estimated traffic of 150.2 vehicles per day (both ways) in the opening season considering that some of the previous categories do not pay the parking and that there are free parking as well. The average speed along the road is 50 km/h.

Besides snow avalanches and other landslide hazards (debris flow in the gullies and flooding along the creeks), the road is also subjected to rockfalls for (almost) its entire length from Bionaz village (Bi in Fig. 3). From previous general studies on the site devoted to land use planning, it results that a total of 6310 m, i.e. from s to e in Fig. 3, are potentially subjected to the hazard. Although a detailed description of the geomorphological context is outlined in Section “Geological knowledge and previous events”, it is anticipated that the areas upstream the road present variegated types of soil and vegetation (loose rock, deposit, grazing, forest), and different slope angles, from gentle slope to overhanging cliffs. Figure 4 shows the different conditions along the road. Even if rockfall risk mitigation measures were installed along the road since its opening (net

Fig. 3 Sketch of the top part of Valpelline valley (Aosta Valley). The road that runs along the valley and links Bionaz (Bi) with Places-Moulin lake (P) is in yellow. The part of road subjected to rockfalls is between *S* and *E* red marks. The major ridges and creeks are marked in black and blue, respectively. The scale marks the kilometers. The map of Italy in the bottom right highlights the position of Aosta Valley

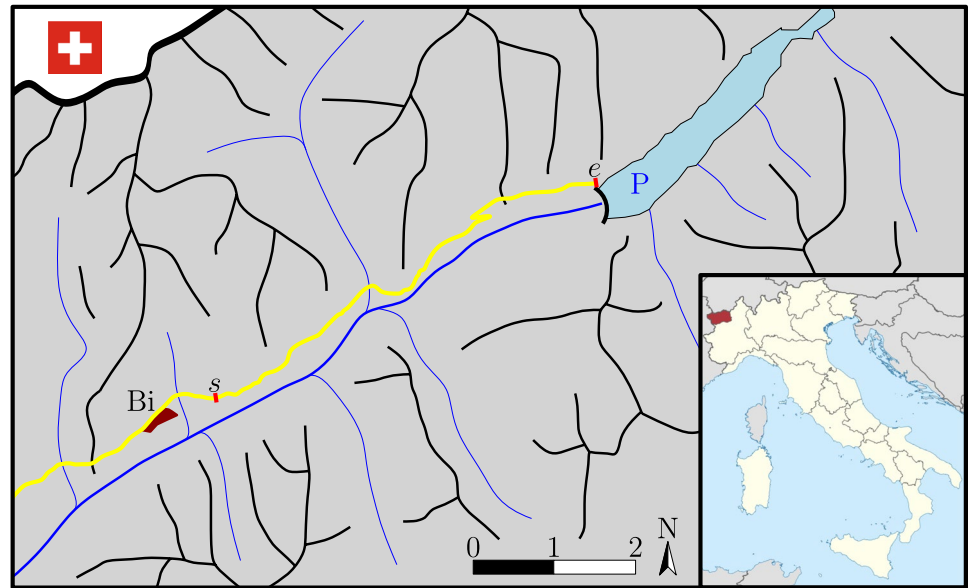


Fig. 4 Three aerial views of the road and the upslope cliffs

fences and drapery meshes), some of them installed in the last 10-15 years. From a detailed survey, it results that some of the net fences are completely rusted and unable to stop blocks, anymore. Several net fences were overturned by the pressure exerted by snow avalanches and, among the drapery meshes, local tearing and lacerations are visible. In general, the information on the original design of the rockfall

protection measures is not available, as well as the knowledge of their efficiency and effectiveness. On the contrary, a few documental information is available on the recent protection works.

The approximate size of the study area is 5.3 km long and approximately 1.5 km wide, i.e. 7.95 km² of surface, with an elevation ranging from 1650 m to 2750 m a.s.l.

Geological knowledge and previous events

From a geological point of view, the Valpelline is made up of tectonic units that, due to their structural position and/or marked lithostratigraphic, chronological and metamorphic affinity, are considered to derive, along with the Southern Alps, from the Adria continental crust which collided against the European plate during the Eocene (Schmid et al. 2004). The Dent Blanche Tectonic System belongs to the Austroalpine domain, derived from the former continental rocks that underwent high-pressure and low-temperature metamorphism (Caso et al. 2024), and is made up of several superimposed tectonic elements: a lower (Mt. Mary–Cervino Nappe) and an upper minor nappes (Dent Blanche s.s.), separated by a mylonitic belt (Roisan–Cignana Shear Zone) (Manzotti et al. 2014). Dent Blanche s.s. nappe, in turn, is formed by two different tectonic units, called series in the traditional literature: the lower is dominated by the presence of gneisses and metagranitoids and the upper with the kinzigitic complex, namely Arolla and Valpelline series, respectively (Dal Piaz et al. 2016). The former is a complex of predominantly orthogneisses with Permian intrusive bodies (granite, diorite, and gabbro), the latter corresponds to the kinzigitic gneisses of the Sesia-Lanzo area and represents a fragment of deep Adriatic crust (Manzotti and Zucali 2013). The studied area comprises rocks of both series: the bottom slopes lies in the Valpelline series, while the higher parts belong to the Arolla series.

The geomorphology of the area is varied with the presence of a main valley, the one of Buthier creek, and several hanging valleys, and it is a direct consequence of rock types, erosive and depositional processes during the evolution of the Western Alps. The dominant shapes are of glacial origin and formed during the multiple phases of glacial expansion and retreat, with an evidence of erosion at the hanging valleys steps (Dal Piaz et al. 2016). It is worth mentioning the collapse of the Becca del Lusency in 1952, which resulted in the collapse of about 1M m³ of rocks and debris from an altitude of 3100 m to the bottom of the valley, causing the death of 4 people (Dutto 1991).

The regional database of past landslide events, available from 1990 and accurately detailed from 2010s, collects, in the majority of the cases, the information referring to (i) the source area, (ii) the total and unitary volumes reaching the road or detached, (iii) unstable already-in-place volumes and (iv) maximum run-out. The regional landslide catalogue reports a total of 11 events along the road in the last 30 years, with volumes reaching the infrastructure ranging from 0.1 to 2 m³.

Based on the geological and geomorphological conditions, coupled with the current knowledge on past events,

7 different road sections were identified. Figure 5 shows an aerial view of the study area with specific indication on the road sections from *s* to *e*, and Table 1 reports the main features of the sections. Section “[Introduction](#)” is characterised by the presence of roadside cut rock walls, as well as a rocky outcrop whose upper edge is positioned at an altitude of 1830 m. There are some protective structures (drapery meshes and rockfall net fences). Section “[Basics of risk calculation on roads](#)” features a detrital slope of mixed origin and covered with grassland (in the lower part used as pastureland with some terracing) from the bottom of the valley to an altitude of approximately 2400 m, corresponding to the top of the slope. The slope has two zones of outcrops: in the lower part, there is a rocky band between 1820 m and 1850 m; in the upper part, there are outcrops arranged along the direction of maximum slope gradient from an altitude of approximately 2100 m to an altitude of 2250 m. Large snow avalanches are observed in this area. Section “[Methodology](#)” is characterised by the presence of numerous walls that could potentially be a source of rockfall. The slope is very high and articulated, with the presence of ledges and gullies that drive the collapse. There are some protective structures (net fences close to the road). Section “[Case study](#)” presents wooded areas and a partially vegetated rockfall deposit. Section “[Discussions](#)” is similar to Section “[Introduction](#)”, with the upper edge of the rocky outcrops at 1900 m and rock walls closer to the road. There are some protective structures (drapery meshes and net fences), and bolts interventions. Section “[Conclusions](#)” features a large detrital stratum, at the top of which (at about 2100 m) there is a compact rocky band that rejoins the south-west slope of the Becca di Châtelet at about 2700 m altitude. The lower part of the slope is locally wooded and used as pastureland. In this road section, the road makes two hairpin bends. The top and medium part of the slope is the propagation area of the snow avalanches that release from Becca di Châtelet. Road section 7 is characterised, in the first part, by an outcrop located at approximately 1980 m, as well as a roadside cut rock wall on which drapery meshes are locally installed. Upstream, the slope presents a rocky ridge, impervious on the west side, partially vegetated on the south-east side. There are rockfall barriers along the road that have suffered numerous impacts. The end, close to the parking area of Places Moulin dam, has some outcrops.

The number of recorded events and collected in the regional landslides database is reported, section-by-section, in the second column of Table 2. The survey carried out along the road showed that the existing rockfall barriers had intercepted and stopped some detached blocks. For the overhanging cliffs secured with drapery meshes, some small volumes were intercepted and retained. During the survey,



Fig. 5 Aerial view of the valley and indication of the seven different road sections. Points *s* and *e* are marked. The letter *C* indicates the top slopes of Becca di Châtelet

Table 1 Main properties of each road section (please refer to Fig. 5)

Section	Length (m)	Altitude (m a.s.l.)	Steepness
1	1215.8	1703–1696	-0.5%
2	427.8	1696–1692	-0.9%
3	809.3	1692–1708	+1.2%
4	377.3	1708–1725	+4.5%
5	1170.6	1725–1810	+7.2%
6	1034.6	1810–1875	+6.2%
7	1267.2	1875–1982	+0.5%

it was found that the slopes that are in snow avalanche hazardous areas (Sections “Basics of risk calculation on roads and Conclusions”) are almost clean of potentially unstable blocks as the avalanche activity promotes the downstream movement of unstable elements. However, some events were recorded in the Regional landslide inventory. In addition, potential instabilities were found. As confirmed by the infrastructure managers, several rockfall events, primarily involving low-volume, single-block detachments, reached the roadway but were not captured in the official Regional landslide inventory, likely due to their limited impact and the absence of systematic survey after severe weather conditions. Drawing on their experience and by comparing the slope conditions with similar rock faces, characterized by comparable lithology, degrees of weathering, and slope angles, in more urbanized areas where higher-resolution data are available, the Authors estimated an average annual frequency of rockfall events, $N_{B,p}$, for each road section, along with the associated likelihood of each estimate. This selection was also guided by observations regarding the number of blocks intercepted by the net fences. Blocks stopped by barriers that were no longer considered effective (showing severe signs of previous damages and ageing, according to Marchelli et al. (2019)) were treated as potential road events. For barriers with unknown installation dates, it was assumed they had been in place for over 25 years, based on certification provided by one of the authors responsible for these protective works. On the contrary, the blocks stopped by the recently installed barriers were not considered in the evaluation of the frequency, assuming that such protection works are effective and correctly designed. To account for the uncertainty, two additional frequencies (and likelihoods) were supposed, as described in Section 3, based on their experience in similar conditions in other sectors of Aosta Valley. In the present analysis, the likelihoods associated with each frequency were determined based on the Authors’ judgment, incorporating insights from rockfall experts (geologists involved in activities in the area) and personnel working at the hydropower dam, who were interviewed during the project. As highlighted in the discussion, alternative approaches are available, including Bayesian updating with expert judgement. The details of frequencies and likelihoods are reported in Table 2.

Table 2 Number of recorded rockfall events and estimated frequencies and likelihoods

Section	Recorded events	Protective structures	$N_{B,p} (yr^{-1})$	$\mathcal{L}_{B,p}$	$N_{B,p}^- (yr^{-1})$	$\mathcal{L}_{B,p}^-$	$N_{B,p}^+ (yr^{-1})$	$\mathcal{L}_{B,p}^+$
1	1	yes	1/2	0.60	0.333	0.10	0.750	0.30
2	0	no	1/10	0.70	0.067	0.20	0.140	0.10
3	1	yes	1/2	0.60	0.333	0.10	0.750	0.30
4	1	no	1/15	0.80	0.044	0.10	0.100	0.10
5	2	yes	1/3	0.60	0.222	0.05	0.495	0.35
6	1	no	1/15	0.50	0.044	0.30	0.100	0.20
7	5	yes	1/2	0.60	0.333	0.05	0.750	0.35

Hazard analysis

As highlighted in the previous sections, due to the size of the studied area, the extent of analysis can be defined as medium-large. As well detailed in Van Westen et al. (2008), for analysis on this kind of scale, the acquisition of detailed spatial data is low applicable, due to excessive economic efforts and the huge practical/computational demand. As a result, detailed geological and geomorphological surveys are generally missing or not achievable. Thus, an accurate identification of the possible source zones, block release probabilities, and involved kinematics cannot be obtained. In these cases, the potential rockfall source areas are generally identified according to the slope angle distribution from high resolution digital elevation model crossed with other information derived from geomorphological and lithological maps (Loye et al. 2009). Steep slopes and rock cliff outcrops frequently merge, being the most probable areas for block detachment. As reported in Section 2, for people travelling along the road, the size of the possible impacting blocks is not a relevant parameter, being all blocks potentially dangerous.

A detailed photogrammetric restitution of the slope was available for selected portions of the study area, acquired in 2023, from which high-resolution DTMs (0.1x0.1 m and 0.5x0.5 m) were generated. These were also resampled to 1x1 m to comply with the requirements of the trajectory simulation software (Dorren 2015), which does not support finer resolutions. The resampled DTMs were carefully aligned with the regional 1x1 m DTM provided by the Local Authority, originally derived from 2018 data and associated with a 2012 orthophoto, to ensure consistency and avoid unrealistic topographic discontinuities. Additionally, Google Earth imagery from 2012, 2014, 2016, and 2023 was consulted to support temporal interpretation of major geomorphological changes. However, due to the lack of multiple high-resolution DTMs covering the entire area, a full terrain-level surface change detection analysis was not feasible. The detailed photogrammetric survey was strategically focused on a large portion of the slope, balancing economic feasibility with spatial coverage. It spans from near the beginning of Section “Introduction” to the boundary

of Section “Conclusions”, and includes an upper portion extending over half of Section 7.

The identification of potential source areas was based on a combination of orthophoto interpretation, field surveys (where accessible), and expert judgment. Structural geological features, such as joint orientation, spacing, and aperture, were analyzed through image-based interpretation and, where possible, supported by preliminary kinematic analyses. Historical inventories of rockfall events and geomorphological indicators, such as talus slopes and scree deposits, further informed the delineation of source zones. In total, 53 source areas were defined and mapped, ranging in size from 500 to 30k m². Terrain analysis techniques were applied using QGIS to support the mapping process, although the final delineation relied heavily on expert interpretation due to the complex geological setting and limited accessibility. Change detection analysis at the scale of individual rockfall events was not feasible, due to the lack of temporally independent high-resolution DTMs or dedicated monitoring systems in the study area. Consequently, volume estimations were not derived from differential surface models but were instead based on geometric approximations informed by field observations and structural analysis.

A preliminary analysis of structural data, historical rockfall events, and visual inspection of deposit areas, supported by engineering and geological judgment, suggests that a block volume of approximately 1 m³ is representative for trajectory analysis. Past events recorded in the catalogue show volume release units (VRUs) ranging from 0.1 m³ to 2 m³, with only one exceptional case exceeding 2 m³. The median volume observed was approximately 0.5 m³. However, it is worth noting that the total volume mobilized during some events was significantly larger, reaching up to 700 m³, indicating that multiple blocks were involved in those cases. Furthermore, the analysis of block deposits near the road, some of which may have been transported by annual avalanche activity, indicates that a volume of 1 m³ corresponds approximately to the 95th percentile of a possible volume size distribution at the location of the element at risk, in line with the recommendations of the Italian Standard UNI 11211-1 (2018). This supports the selection of 1 m³ as a representative block size for trajectory analyses.

It is worth noting that the proposed risk assessment methodology in this case does not rely on estimating detachment probabilities or volumes directly at the source areas. Instead, it focuses on the frequency of blocks arrived at the location of the elements at risk, informed by the catalogue of past events and field surveys of deposit zones, including the existing protection works. Consequently, trajectory analyses were performed to assess which sub portions and thus portions of each slope section, defined as homogeneous in terms of event frequency, are more likely to be affected by block arrival. Recognizing thus that trajectory outcomes can vary with block size (except in purely lumped-mass models), simulations were conducted using two representative volumes: 0.5 m^3 and 1 m^3 . By simulating two representative block volumes and adopting the worst-case envelope, the method reduces somehow the epistemic uncertainty by accounting for variability in block behaviour without requiring precise knowledge of block size at the impact location. Trajectory analyses to identify interactions between rockfall and infrastructure were carried out using the 3D hybrid model implemented in Rockyfor3D (Dorren 2015), which simulates ground–rock interactions based on block shape while modelling free-fall phases using a lumped-mass approach (Raibaut et al. 2025). Notably, in the simulated case, the model did not exhibit significant differences in block behaviour between the two tested volumes (0.5 m^3 and 1 m^3), supporting the robustness of the selected representative block size and contributing to the reduction of epistemic uncertainty. In Rockyfor3D, block–slope interactions are modelled using restitution coefficients that reflect terrain properties. The normal restitution coefficient is assigned based on soil type, which is mapped in the field and linked to predefined elasticity values. To reduce aleatory uncertainty, the tangential restitution coefficient is dynamically calculated using the block radius, penetration depth, and macro-roughness, i.e. the size of surface obstacles like rocks recorded as mean obstacle heights in three probabilistic classes (rg70, rg20, rg10). Since the model uses random sampling from these classes during each rebound, this approach primarily addresses aleatory uncertainty, capturing the inherent variability in terrain conditions and their influence on block trajectories. In the present case, the classification of soil types and macro-roughness was based on a combination of field surveys and image interpretation, allowing for the delineation of homogeneous terrain units across the study area. To improve the reliability of the input parameters, these classifications were further calibrated through back-analysis of three well-documented past rockfall events occurring in different zones of the study area. The first event, in 1991, involved a VRU of approximately 1 m^3 and a total mobilised volume of 80 m^3 . Both the source area and the distribution of deposited blocks along the road were

well documented. The second event, in 2012, had a mean VRU of 0.2 m^3 and a total volume between 10 and 30 m^3 , with similarly detailed data available for both the detachment and blocks arrived on the road. The third event, in 2014, provided not only information on source and deposit areas but also detailed observations of the block trajectories and impact points, which were used to refine the restitution parameters. These back-analyses ensured that the restitution coefficients used in the model reflect realistic block–terrain interactions under site-specific conditions.

Figure 6.a displays the results of the propagation analyses in terms of reach probability in each cell of the DEM. In cases in which multiple source zones insist on the same section, precautionary, the envelope of the results was taken as representative. To provide a wider overview of the hazard in the area, the rockfall mitigation measures were not modelled in the analysis as (i) it allows checking which areas are more prone to the hazard, independently from the protection systems, and (ii) it considers the hazard if the net fences are not efficient.

Risk analysis

The risk analysis is based on the annual frequency of events on the road sections. Table 2 reports such information. The probability of having, at least, one rockfall event along each sub-portion of the road can be computed thanks to Eq. (8) once the annual frequency along each section is split in the sub-portions based on the reach probability, as for Eq. (6). Figure 6.b reports the annual probability of having, at least, one rockfall occurrence in each sub-portion of the road, namely $P_{(S:T)}(1\text{yr})$ computed with the estimated rockfall annual frequencies in each section reported in the fourth-column of Table 2, i.e. $N_{B,p}$.

The difference between the reaching probability obtained from the propagation analysis, which is atemporal, and the annual probability of (at least) one occurrence is clearly visible. It could be observed that some areas with high reach probability can experience a low annual occurrence probability due to a low annual frequency of events. This is the case, for example, of the hairpin bends in Section “Conclusions”. The knowledge of both information (reach probability and annual probability) is useful for policy-makers to evaluate the most critical areas and prioritize the interventions.

The quantification of the risk assessment for road users was performed according to the procedures explained in Section “Basics of risk calculation on roads”. The parking area was not considered in the present analysis as large protection works have been recently built. Table 3 reports the input parameters adopted for the analyses. Referring to the probabilities required by the ETA (refer to Fig. 1 for

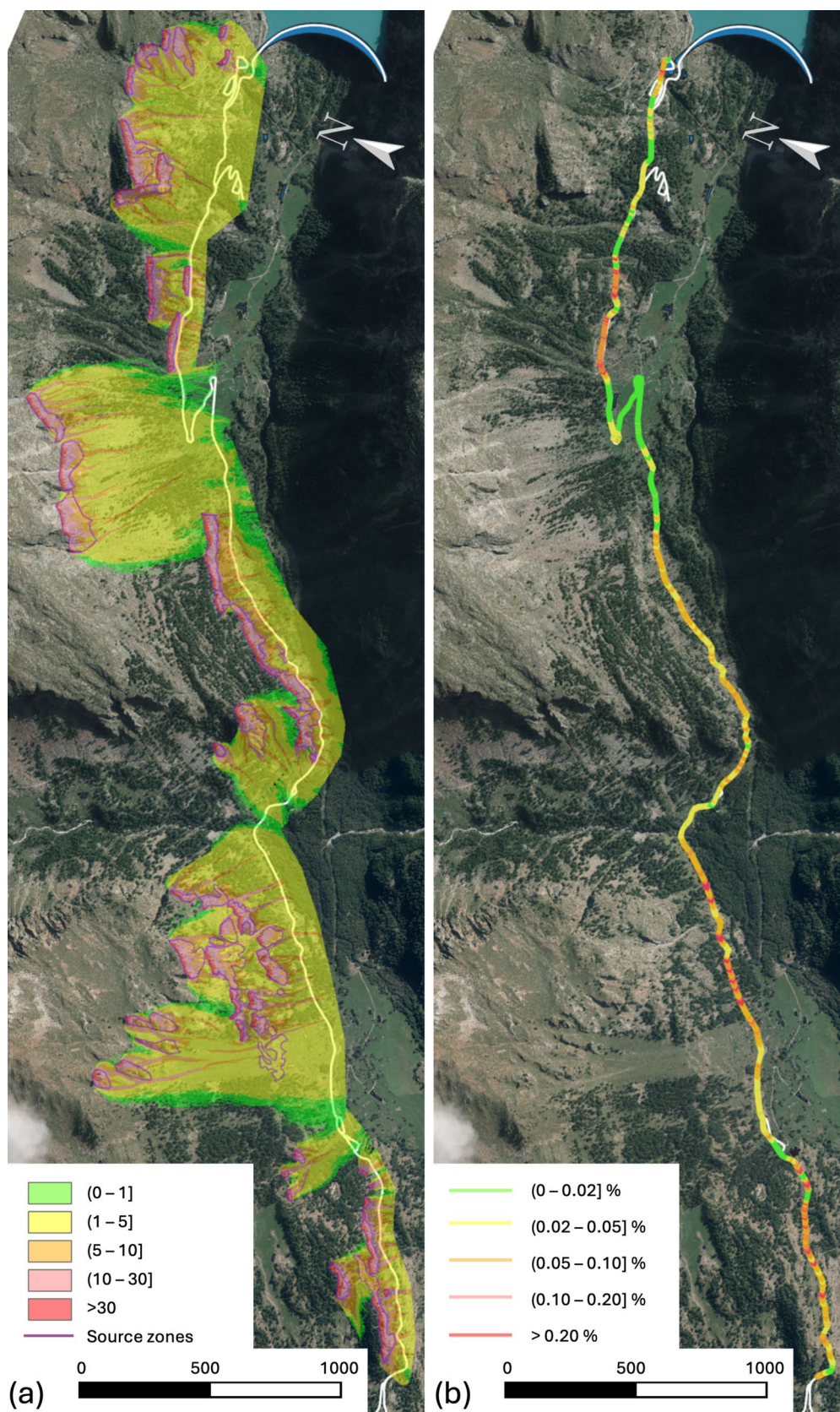


Fig. 6 (a) Aerial view of the area with overlaid the source zones and the reach probability $P_{(S:B)}$ (in %) obtained from the trajectory analysis. (b) Annual probability of having, at least, one rockfall occurrence in each sub-portion of the road considering $N_{B,p}$ occurrences according to Table 2

Table 3 Input data for the assessment of the risk for the road and the parking area

Input data	
Number of vehicles	32000
Velocity of the vehicles	50 km/h
Length of the vehicle	5 m
Number of people/vehicle	≥ 3
Annual operation duration (213 days)	5110 hrs
$P_{i,fatal}$	0.2
P_f	0.5
$P_{s,fatal}$	0.041
P_t	0.2
$P_{d,fatal}$	0.026

symbols), the probability that a block stops or rebounds on the infrastructure was computed through the trajectory analyses, while P_t , $P_{s,fatal}$, and $P_{d,fatal}$ were estimated from the Italian Statistics of road accidents due to the presence of obstacles or due to pavement issues. The number of vehicles, their speed and the operational period of the road (April to October) derives from the description of the site detailed at the beginning of Section “Case study”. As stated in Section “Methodology”, in this study, the assumption that any block impact is damaging is applied when exposure is already accounted for (i.e. the vehicle is present in the hazard zone), and a 20% probability of fatality is assigned to such impacts ($P_{i,fatal}$), following a conservative yet evidence-based approach (Bunce et al. 1997).

Following the approach reported in Section “Methodology”, the risk was computed for $3^7 = 2187$ different combinations of the occurrence frequencies in the seven road sections. Table 4 reports the calculation for the first two, and the last combinations. To each set of frequencies, the associated likelihoods and the computed risk are reported. The total risk on the entire road related to this combination of occurrence frequencies is the sum of the single risks (the

Table 5 Calculation of the cumulative likelihood, i.e. the probability of having a risk smaller than R

$R (\times 10^7)$	\mathcal{L}	$P(r \leq R)$
27.9	0.0000002	0.0000002
28.4	0.0000012	0.0000014
28.4	0.0000003	0.0000016
28.6	0.0000005	0.0000021
28.8	0.0000020	0.0000041
29.0	0.0000002	0.0000043
61.4	0.0004410	0.9995369
61.6	0.0000331	0.9995700
61.6	0.0000221	0.9995921
61.7	0.0001544	0.9997464
62.1	0.0001764	0.9999228
62.1	0.0000551	0.9999779
62.7	0.0000221	1.0000000

risk values are multiplied times 10^7 to reduce the width of the table), while the likelihood of such risk is the product of the likelihoods of each section. It must be noted that the sum of the likelihoods obtained for the all the combinations is one.

The 2178 risk values were sorted from the smallest to the largest, and the likelihoods were progressively summed to obtain a cumulative probability distribution. Table 5 reports an excerpt of the analysis. The third column is the cumulative summation of the likelihoods. It clearly appears that the third column is the probability of having a risk r smaller than a given value, i.e. $P(r \leq R)$. Finally, Figure 7 depicts, in blue (continuous line), the curve obtained considering that the traffic along the road is about 32k vehicles per year. The same analysis was replicated for other traffic conditions, i.e. 40k, 50k, and 60k vehicles per year, to measure the impact on the risk of a potential touristic development of the area. The obtained curves are reported in red, yellow and violet (continuous lines) in Fig. 7. The values of the risk

Table 4 Societal risk calculation for different occurrence frequencies in the seven road sections. Each macro-row corresponds to a combination of the occurrence parameters. Cases #1 and #2 differs with respect to the occurrence parameter in Section 7

#		Section “Introduction”	Section “Basics of risk calculation on roads”	Section “Methodology”	Section “Case study”	Section “Discussions”	Section “Conclusions”	Section 7	Entire road
1	$N_{B,p}$	0.5	0.1	0.5	0.067	0.333	0.067	0.5	
	$\mathcal{L}_{B,p}$	0.6	0.7	0.6	0.8	0.6	0.5	0.6	0.0362880
	$R_p (\times 10^7)$	10.1	2.0	10.1	1.4	6.8	1.4	10.1	41.9
2	$N_{B,p}$	0.5	0.1	0.5	0.067	0.333	0.067	0.05	
	$\mathcal{L}_{B,p}$	0.6	0.7	0.6	0.8	0.6	0.5	0.333	0.0030240
	$R_p (\times 10^7)$	10.1	2.0	10.1	1.4	6.8	1.4	6.8	38.5
2187	$N_{B,p}$	0.75	0.15	0.75	0.1	0.495	0.1	0.75	
	$\mathcal{L}_{B,p}$	0.3	0.1	0.3	0.1	0.35	0.2	0.35	0.0000221
	$R_p (\times 10^7)$	15.2	3.0	15.2	2.0	10.0	2.0	15.2	62.7

Fig. 7 Risk vs. cumulative likelihood curves for different annual traffic conditions. The continuous lines refer to the risk computed considering the input data of Table 3, while dashed curves relate to the 90% confidence bounds, as detailed in Section “Discussions”

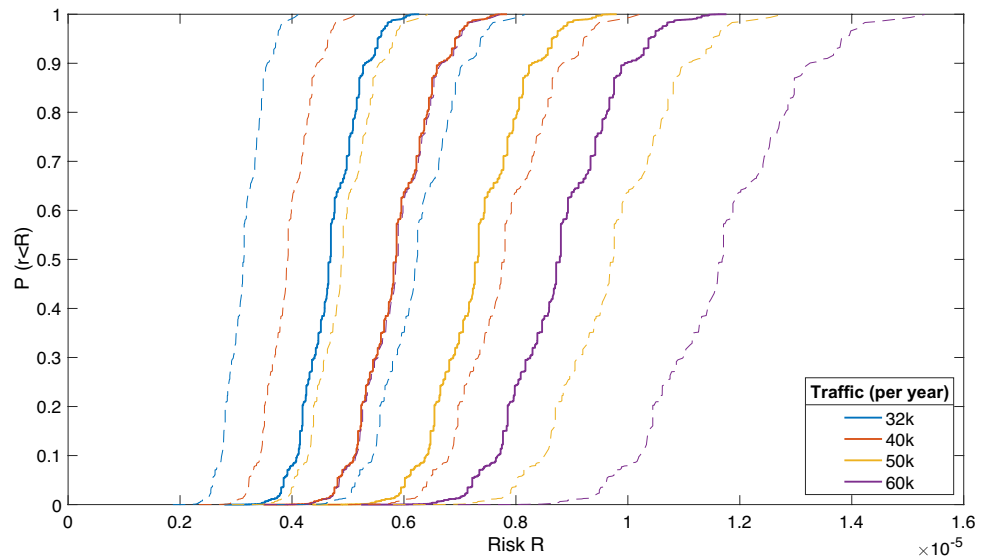


Table 6 Values of R corresponding to 50- and 90-percentiles for the different traffic scenarios analyzed

Traffic (per yr)	$R P(r \leq R) = 0.5$	$R P(r \leq R) = 0.9$
32k vehicles	4.68×10^{-6}	5.36×10^{-6}
40k vehicles	5.86×10^{-6}	6.66×10^{-6}
50k vehicles	7.32×10^{-6}	8.23×10^{-6}
60k vehicles	8.78×10^{-6}	9.97×10^{-6}

R corresponding to 50- and 90-percentiles are reported in Table 6.

Discussions

The analysis indicates that the societal risk, computed as the probability of having at least one fatality per year, along the road is smaller than 1×10^{-5} . This value has been computed considering that only the effective net fences are able to intercept and stop the falling blocks, while the old barriers are neglected. Results in terms of hazard and risk are both useful to define management strategies, to identify the portions of the very large area that need detailed analyses, and, eventually, to design and install additional mitigation measures. First, the obtained risk values should be compared to an acceptable threshold and, if higher, risk reduction plans should be evaluated. For societal risk, the Italian Standard UNI 11211-2 (2021) suggests to consider a value in between 10^{-6} and 10^{-5} per year as reasonably acceptable in case of rockfall protected structures or infrastructures. However, it must be noted that the value of such threshold is still under debate in the scientific community (Enright 2015; Sim et al. 2022). To the knowledge of the Authors, a predefined value has not been defined yet.

The map of the reach probability, $P_{(S:B)}$, shown in Fig. 6.a, is useful for managing risk. It helps identify which source areas impact longer stretches of road and, therefore, may pose a greater risk to exposed elements. This information can be used to determine where preventive measures should be prioritised or checking if the current protection structures are located in the optimal position. Figure 6.b, on the other hand, presents the annual probability of at least one occurrence. This map complements that in Fig. 6.a, as it highlights the most critical zones where blocks are more likely to arrive, incorporating temporal information. As a result, the values shown may not necessarily coincide with those in the reach probability map. This map supports the identification of areas where protective measures should be prioritised. Naturally, this map can only be produced when a catalogue of past events is available.

Analysing then the sources of uncertainty, it should be noticed that the core of the procedure for risk quantification lies on the definition of the number of events along the infrastructure. Hence, the approach implicitly accounts for uncertainties in all processes along the slope, from detachment to propagation, including potential fragmentation. The epistemic uncertainty in the definition of the number of events has been solved by introducing a likelihood of having a certain frequency of occurrence. To assess how effectively the method captures uncertainties in estimating the occurrence

Table 7 Risk computed considering no uncertainties in the occurrences, Q , and minimum and maximum risks considering the uncertainties, for the different analysed traffic scenarios. The right-hand side column reports the risks in case the protective structures would be not effective

Traffic (per yr)	No uncertainties, Q	min R	max R	No net-fences, U
32k vehicles	4.73×10^{-6}	2.79×10^{-6}	6.27×10^{-6}	6.02×10^{-6}
40k vehicles	5.91×10^{-6}	3.49×10^{-6}	7.84×10^{-6}	7.51×10^{-6}
50k vehicles	7.39×10^{-6}	4.36×10^{-6}	9.80×10^{-6}	9.39×10^{-6}
60k vehicles	8.87×10^{-6}	5.24×10^{-6}	11.76×10^{-6}	1.13×10^{-5}

of the phenomenon, Table 7 also reports the annual risk values obtained by assuming that the frequencies $N_{B,p}$ have unit likelihood, i.e. no uncertainties are considered. Such values, named as Q , can be compared with the minimum and maximum risks, as well with the risks corresponding to specific percentiles, say 50th and 90th, reported in Table 6. The results show that, irrespectively from the annual traffic, the risk computed under this assumption approximately corresponds to the 50th percentile of the empirical distribution of risk and likelihoods. The range of the computed risks, i.e. ($\max R - \min R$), is progressively increasing, from 3.48×10^{-6} at 32k vehicles per year, to 6.52×10^{-6} at 60k vehicles per year.

The probability of a fatal accident, i.e. PF in Eq. (1), primarily influenced by the vehicle's velocity and the number of occupants, can increase or decrease depending on the average speed on the infrastructure and the average number of occupants per vehicle. As reported in the literature, vehicle velocity varies significantly, especially on mountain roads (Andueza 2000; Nama et al. 2016). To account for parameter variability, a coefficient of variation of 0.2 relative to the mean values of the individual probability of fatality is considered. The error is propagated from the individual probability to the overall probability of fatality, PF^k of Eq. (10), according to the number of vehicles. Figure 7 presents the 90% confidence bounds of the risk-likelihood curves. As expected, the bounds widen as the number of vehicles increases; at $P(r < R) = 0.5$, the widths of the bounds are 3.1×10^{-6} , 3.88×10^{-6} , 4.85×10^{-6} and 5.82×10^{-6} , for 32, 40, 50, and 60 thousands vehicles, respectively.

Finally, to assess the risk in the event that the net fences, previously considered effective, fail to intercept and stop the blocks, the risk was recalculated for the four traffic scenarios. The number of events on those Sections in which protection systems are installed (1, 3, 5 and 7) was determined based on the surveys performed by the Authors along the road. The considerations relate to the barriers that have been recently installed, only, as the protection provided by the older and not efficient ones has been discarded in the calculations. To quantify the extra blocks reaching the road, it has been considered that the barriers have been installed, on average, 10 years ago. This means that the

blocks accumulated behind the barrier were added to the list of blocks that reached the road in a 10 years period. The updated frequencies $N_{B,p}$ is 0.50, 0.70, 0.50, 0.60, for Sections "Introduction", "Methodology", "Discussions" and 7, respectively and the corresponding risks are reported in the right-hand side column of Table 7. Here, a unit likelihoods is associated to each frequency. These risks refer to the case in which maintenance of the barriers is no longer performed and the current mitigation measures undergo ageing and severe degradation.

Referring to the obtained likelihood, looking at other methods, such figure can be intended as a prior distribution in a Bayesian inference analysis. In fuzzy risk analysis, a probability is attributed to the feasibility of a value of an input variable. The approach is similar to the one proposed by the Authors. It is worth noting that the likelihood associated to the possible occurrence frequencies that can be assigned to a specific road section can result from independent evaluations of a pool of experts. For example, each expert could be asked to indicate what they think is the likely frequency of occurrence (from a range of predefined frequencies). The results of the survey would provide the likelihoods to be incorporated into the risk analysis. However, it is important to remind that missing events can have relevant consequences when the frequency of occurrence is taken as input for additional analyses (De Biagi 2017): hence, attention must be provided to the evaluation of this parameter.

Implications and recommendation

The results of the analyses provide a coherent and quantitative framework for understanding the rockfall hazard affecting the study area and potential consequences, with direct implications for road management and territorial planning. The presence of numerous potential rockfall sources, combined with the steep morphology of the slopes, results in a significant spatial probability of block reach in the event of detachment. This condition is particularly critical in the absence of detailed information on existing protective structures, which can also not be considered in the modelling due to the lack of design documentation and the heterogeneous state of conservation observed during field inspections. The

seasonal increase in vehicular and pedestrian traffic, especially during the summer months, further amplifies the vulnerability of the road infrastructure and adjacent rest areas. The mapping of annual reaching probability, which accounts for the variability in rockfall frequency along different road segments, allows for a more refined risk assessment and supports the prioritisation of intervention strategies.

In light of these findings, it is recommended to improve the geological characterisation of the rock masses through targeted field investigations, including rope-access surveys and volumetric assessments of potentially unstable blocks, with particular attention to source areas that could affect extensive segments of the road, as can be inferred from Fig. 6.a. Among the possible mitigation strategies, and specifically considering structural measures, the installation of net fences emerges as a potentially profitable solution. These systems can be designed with tailored energy absorption capacity and height, based on detailed trajectory analyses, to effectively intercept falling blocks. This approach is preferable to secured drapery meshes and rock bolting on the potential unstable zones, due to the extensive nature of the potential source areas, which limits the effectiveness of localised stabilisation techniques. Given the available financial resources, the map integrating both the probability of reach and the frequency of events, i.e. Figure 6.b, could provide a cost-effective basis for prioritizing areas for protection. Considering the potential block volumes reaching the road (VRU equal to 1 m^3), embankments, although generally reliable for withstanding multiple impacts and requiring minimal maintenance, may prove economically unfeasible in this context. Nevertheless, a systematic and long-term evaluation of the condition of all the protective (or preventive) structures, both existing and future, should be undertaken to support maintenance planning and ensure continued effectiveness over time (Marchelli et al. 2019, 2020b, 2022b). Furthermore, considering non-structural measures, traffic management can act as a non-structural risk mitigation measure. The maximum allowable number of vehicles per day can be fixed, based on risk threshold. It is also advisable to regulate access to the road during periods of intense rainfall, which are known to increase the likelihood of rockfall events (Delonca et al. 2014; D'Amato et al. 2016). Finally, prior to the seasonal reopening of the road, inspections should be carried out to identify and remove any unstable blocks. These measures aim to enhance the safety and resilience of the infrastructure while supporting the sustainable use of the area.

Conclusions

A specific request from a Public Administration led to the design of a new methodology to quantify rockfall societal risk along a 7.5 km road in the particular case in which there

is limited knowledge of the area. The risk is computed following the procedure illustrated by the Authors in Marchelli (2020); Marchelli et al. (2022a), which requires details on traffic conditions (number of vehicles, speed, etc.) and on the occurrence of rockfall events along the road. The former point can be easily estimated by measuring the current traffic, or by proposing new scenarios based on the expected urban-touristic development of the area. The latter, which is directly linked to the hazardous phenomenon, can be defined in probabilistic terms, by considering different occurrence frequencies and associating to each of them a likelihood, i.e. a probability that measures the degree of expectation, corresponding to a prior probability in a Bayesian approach. The occurrences and the corresponding likelihoods are determined from the analysis of the inventory of past events enriched with the information taken from on-site survey (from protection structures, damaged elements, etc.). The output of the process consists in a set of values of risk and associated likelihoods. The risk corresponding to a specific percentile serves as basis for risk management. In addition, two maps define the areas in which detailed analyses are needed. The limitations of the procedure and the sources of uncertainty have been discussed. The procedure is suitable to be implemented in risk analyses when limited knowledge is present, taking care of the limitations and the implications of the hypotheses done.

Author Contribution MM: Conceptualization, Methodology, Formal analyses, Writing - original draft, Writing - Review & Editing, Project administration, Funding acquisition. VDB: Conceptualization, Methodology, Formal analyses, Writing - original draft, Writing - Review & Editing, Project administration, Funding acquisition. MP: Conceptualization, Data acquisition, Writing - Review & Editing, Project administration. DB: Conceptualization, Data acquisition, Project administration.

Funding Open access funding provided by Politecnico di Torino within the CRUI-CARE Agreement. This work was partially supported by the research project "Servizio di supporto altamente specialistico al Responsabile Unico del Procedimento nell'ambito della predisposizione di strumenti per la gestione del rischio da caduta massi su insediamenti abitativi e della valutazione de rischio su strade ad alta vulnerabilità" funded by Regione Autonoma Valle d'Aosta (Italy) and partially by the Marie Curie Postdoctoral Fellowship 2022 (Call Horizon-MSCA-2022-PF-01, Grant GA101103401 (RIDETHERISK project).

Open Access This article is licensed under a Creative Commons Attribution 4.0 International License, which permits use, sharing, adaptation, distribution and reproduction in any medium or format, as long as you give appropriate credit to the original author(s) and the source, provide a link to the Creative Commons licence, and indicate if changes were made. The images or other third party material in this article are included in the article's Creative Commons licence, unless indicated otherwise in a credit line to the material. If material is not included in the article's Creative Commons licence and your intended use is not permitted by statutory regulation or exceeds the permitted use, you will need to obtain permission directly from the copyright holder. To view a copy of this licence, visit <http://creativecommons.org/licenses/by/4.0/>.

References

- Abaker M, Dafaalla H, Eisa TAE et al (2023) Deep learning-and iot-based framework for rock-fall early warning. *Appl Sci* 13(17):9978
- Agliardi F, Crosta GB (2003) High resolution three-dimensional numerical modelling of rockfalls. *Int J Rock Mech Min Sci* 40(4):455–471
- Al-Shaar M, Gerard PC, Faour G, et al (2024) A comprehensive approach to quantitative risk assessment of rockfalls on buildings using 3d model of rockfall runout. *J* 7(2):183–203
- Andueza PJ (2000) Mathematical models of vehicular speed on mountain roads. *Transportation Research Record* (1701)
- Aven T (2008) A semi-quantitative approach to risk analysis, as an alternative to qras. *Reliability Engineering & System Safety* 93(6):790–797
- Beven KJ, Almeida S, Aspinall WP et al (2018) Epistemic uncertainties and natural hazard risk assessment-part 1: a review of different natural hazard areas. *Nat Hazard* 18(10):2741–2768
- De Biagi V (2017) Brief communication: accuracy of the fallen blocks volume-frequency law. *Nat Hazard* 17(9):1487–1492
- De Biagi V, Napoli ML, Barbero M et al (2017) Estimation of the return period of rockfall blocks according to their size. *Nat Hazard* 17(1):103–113
- De Biagi V, Marchelli M, Peila D (2020) Reliability analysis and partial safety factors approach for rockfall protection structures. *Eng Struct* 213:110553
- Budetta P, De Luca C, Nappi M (2016) Quantitative rockfall risk assessment for an important road by means of the rockfall risk management (ro. ma.) method. *Bull Eng Geol Env* 75:1377–1397
- Bunce C, Cruden D, Morgenstern N (1997) Assessment of the hazard from rock fall on a highway. *Can Geotech J* 34(3):344–356
- Bunce C, Cruden D, Morgenstern N (1997) Assessment of the hazard from rock fall on a highway. *Can Geotech J* 34(3):344–356
- Cardenas IC, Aven T, Flage R (2022) Addressing challenges in uncertainty quantification. the case of geohazard assessments. *Geoscientific Model Development Discussions* 2022:1–23
- Caso F, Piloni C, Filippi M et al (2024) Combining traditional and quantitative multiscale structural analysis to reconstruct the tectono-metamorphic evolution of migmatitic basements: the case of the valpelline series, dent-blanche tectonic system, western alps. *J Struct Geol* 182:105099
- Chanut MA, Courteille H, Lévy C et al (2024) Managing rockfall hazard on strategic linear stakes: how can machine learning help to better predict periods of increased rockfall activity? *Sustainability* 16(9):3802
- Chen G, Zheng L, Zhang Y et al (2013) Numerical simulation in rockfall analysis: a close comparison of 2-d and 3-d dda. *Rock Mech Rock Eng* 46(3):527–541. <https://doi.org/10.1007/s00603-012-0360-9>
- Corominas J, van Westen C, Frattini P et al (2014) Recommendations for the quantitative analysis of landslide risk. *Bull Eng Geol Env* 73:209–263
- Crosta G, Agliardi F (2004) Parametric evaluation of 3d dispersion of rockfall trajectories. *Nat Hazard* 4(4):583–598
- D'Amato J, Hantz D, Guerin A et al (2016) Influence of meteorological factors on rockfall occurrence in a middle mountain limestone cliff. *Nat Hazard* 16(3):719–735
- Dal Piaz GV, Bistacchi A, Gianotti F, et al (2016) Note illustrative del f. 070 monte cervino della carta geologica d'italia alla scala 1: 50.000. In: *Note Illustrative del F. 070 Monte Cervino della Carta Geologica d'Italia alla scala 1: 50.000, vol 101. ISPRA-Servizio Geologico d'Italia*, p 1–272
- Delonca A, Gunzburger Y, Verdel T (2014) Statistical correlation between meteorological and rockfall databases. *Nat Hazard* 14(8):1953–1964
- De Ru WG, Eloff JH (1996) Risk analysis modelling with the use of fuzzy logic. *Computers & Security* 15(3):239–248
- Dorren LK (2003) A review of rockfall mechanics and modelling approaches. *Prog Phys Geogr* 27(1):69–87
- Dorren L (2015) Rockyfor3d (v5. 2) revealed—transparent description of the complete 3d rockfall model. *EcorisQ paper* (www.ecorisq.org)
- Dussauge C, Grasso JR, Helmstetter A (2003) Statistical analysis of rockfall volume distributions: Implications for rockfall dynamics. *Journal of Geophysical Research: Solid Earth* 108(B6)
- Dutto F (1991) Grandi frane con percorso su ghiacciaio in valle d'aosta. *Revue Valdotaïne d'Histoire Naturelle* 45:21–35
- Enright P (2015) Is there a tolerable level of risk from natural hazards in new zealand? *Georisk: Assessment and Management of Risk for Engineered Systems and Geohazards* 9(1):1–8
- Fanos AM, Pradhan B, Alamri A et al (2020) Machine learning-based and 3d kinematic models for rockfall hazard assessment using lidar data and gis. *Remote Sensing* 12(11):1755
- Farmakis I, DiFrancesco PM, Hutchinson DJ et al (2022) Rockfall detection using lidar and deep learning. *Eng Geol* 309:106836
- Farmakis I, Guccione DE, Thoeni K et al (2025) Voxfall: non-parametric volumetric change detection for rockfalls. *Eng Geol* 352:108045
- Farmer M, Weir F, Fowler M, et al (2023) A qualitative rockfall hazard screening tool for open pit mining. In: *SSIM 2023: Third International Slope Stability in Mining Conference*, Australian Centre for Geomechanics, pp 649–662
- Farvacque M, Corona C, Lopez-Saez J, et al (2021) Estimating rockfall release frequency from blocks deposited in protection barriers, growth disturbances in trees, and trajectory simulations. *Landslides* pp 1–12
- Favillier A, Mainieri R, Saez JL, et al (2017) Dendrogeomorphic assessment of rockfall recurrence intervals at saint paul de varces, western french alps. *Géomorphologie: relief, processus, environnement* 23(2)
- Fell R, Corominas J, Bonnard C et al (2008) Guidelines for landslide susceptibility, hazard and risk zoning for land use planning. *Eng Geol* 102(3–4):85–98
- Fell R, Ho KK, Lacasse S, et al (2005) A framework for landslide risk assessment and management. In: *Landslide risk management*. CRC Press, p 13–36
- Feng L, Intrieri E, Pazzi V et al (2021) A framework for temporal and spatial rockfall early warning using micro-seismic monitoring. *Landslides* 18:1059–1070
- Fenton N, Neil M (2018) Risk assessment and decision analysis with Bayesian networks. *Crc Press*
- Ferrari F, Giacomini A, Thoeni K (2016) Qualitative rockfall hazard assessment: a comprehensive review of current practices
- Hantz D, Vengeon J, Dussauge-Peisser C (2003) An historical, geomechanical and probabilistic approach to rock-fall hazard assessment. *Nat Hazard* 3(6):693–701
- Hantz D, Dewez T, Lévy C et al (2016) Rockfall frequency in different geomorphological conditions. *International Symposium Rock Slope Stability 2016*:1–2
- Hantz D, Corominas J, Crosta GB et al (2021) Definitions and concepts for quantitative rockfall hazard and risk analysis. *Geosciences* 11(4):158
- He R, Zhang W, Dou J, et al (2024) Application of artificial intelligence in three aspects of landslide risk assessment: A comprehensive review. *Rock Mechanics Bulletin* p 100144
- Hoek E, Karakas A (2008) Practical rock engineering. *Environ Eng Geosci* 14(1):55–58
- Hungr O, Evans S, Hazzard J (1999) Magnitude and frequency of rock falls and rock slides along the main transportation corridors of southwestern british columbia. *Can Geotech J* 36(2):224–238

- Hwang IT, Lee JH, Pradhan AMS et al (2024) Probabilistic back analysis for landslide susceptibility assessment in data-scarce regions using a bayesian approach. *Geomat Nat Haz Risk* 15(1):2434616
- Jonkman S, Van Gelder P, Vrijling J (2003) An overview of quantitative risk measures for loss of life and economic damage. *J Hazard Mater* 99(1):1–30
- Kaikkonen L, Parviainen T, Rahikainen M et al (2021) Bayesian networks in environmental risk assessment: a review. *Integr Environ Assess Manag* 17(1):62–78
- Kanno H, Moriguchi S, Tsuda Y et al (2023) A method for rockfall risk quantification and optimal arrangement of protection structures along a road. *Eng Geol* 314:107004
- Lan H, Martin CD, Zhou C et al (2010) Rockfall hazard analysis using lidar and spatial modeling. *Geomorphology* 118(1–2):213–223
- Lempert RJ, Groves DG, Popper SW et al (2006) A general, analytic method for generating robust strategies and narrative scenarios. *Manage Sci* 52(4):514–528
- Li L, Lan H (2015) Probabilistic modeling of rockfall trajectories: a review. *Bull Eng Geol Env* 74:1163–1176
- Loye A, Jaboyedoff M, Pedrazzini A (2009) Identification of potential rockfall source areas at a regional scale using a dem-based geomorphometric analysis. *Nat Hazard* 9(5):1643–1653
- Macciotta R (2023) Slope risk management in light of uncertainty and environmental variability-2021 canadian geotechnical colloquium. *Can Geotech J* 60(12):1777–1791
- Macciotta R, Martin CD, Cruden DM (2015) Probabilistic estimation of rockfall height and kinetic energy based on a three-dimensional trajectory model and monte carlo simulation. *Landslides* 12:757–772
- Macciotta R, Martin C, Morgenstern N et al (2016) Quantitative risk assessment of slope hazards along a section of railway in the canadian cordillera—a methodology considering the uncertainty in the results. *Landslides* 13(1):115–127
- Macciotta R, Martin CD, Morgenstern NR et al (2016) Quantitative risk assessment of slope hazards along a section of railway in the canadian cordillera—a methodology considering the uncertainty in the results. *Landslides* 13:115–127
- Macciotta R, Martin CD, Cruden DM, et al (2017) Rock fall hazard control along a section of railway based on quantified risk. *Georisk: Assessment and Management of Risk for Engineered Systems and Geohazards* 11(3):272–284
- Macciotta R, Gräpel C, Keegan T et al (2020) Quantitative risk assessment of rock slope instabilities that threaten a highway near canmore, alberta, canada: managing risk calculation uncertainty in practice. *Can Geotech J* 57(3):337–353
- Maheshwari S, Bhowmik R, Samanta M (2023) Rockfall hazard: a comprehensive review of current mitigation practices. *Landslides: detection, prediction and monitoring: technological developments* pp 175–209
- Manzotti P, Zucali M (2013) The pre-alpine tectonic history of the austroalpine continental basement in the valpellina unit (western italian alps). *Geol Mag* 150(1):153–172
- Manzotti P, Zucali M, Balleve M et al (2014) Geometry and kinematics of the roisan-cignana shear zone, and the orogenic evolution of the dent blanche tectonic system (western alps). *Swiss J Geosci* 107:23–47
- Marchelli M (2020) Event tree analysis for mountain roads under rockfall hazard. *GEAM Geingegneria Ambientale E Mineraria* 161:41–46
- Marchelli M, De Biagi V, Peila D (2019) A quick-assessment procedure to evaluate the degree of conservation of rockfall drapery meshes. *Frattura ed Integrità Strutturale* 13(47):437–450
- Marchelli M, Biagi VD, Peila D (2020a) Reliability-based design of protection net fences: influence of rockfall uncertainties through a statistical analysis. *Geosciences* 10(8):280
- Marchelli M et al (2020b) Una procedura speditiva per la valutazione dello stato di conservazione delle barriere paramassi a rete. *GEAM Geingegneria Ambientale e Mineraria* pp 24–35
- Marchelli M, De Biagi V, Peila D (2021) Reliability-based design of rockfall passive systems height. *Int J Rock Mech Min Sci* 139:104664
- Marchelli M, De Biagi V, Bertolo D et al (2022a) A mixed quantitative approach to evaluate rockfall risk and the maximum allowable traffic on road infrastructure. *Georisk: Assessment and Management of Risk for Engineered Systems and Geohazards* 16(3):584–594
- Marchelli M, Paganone M, Bertolo D et al (2022b) A tool for monitoring rockfall protection works and plan the maintenance: the case of the autonomous region of valle d'aosta. *GEAM GEOINGEGNERIA AMBIENTALE E MINERARIA* 166:33–41
- Marchelli M, Guccione DE, Giacomini A, Buzzi O (2025) Fragmentation patterns and trajectories during rockfall: analysis of the influence of discontinuities and impact conditions through drop tests. In: Marchelli M et al (eds) *Rock Mech Rock Eng*, pp 1–33. Marchelli 2025. <https://doi.org/10.1007/s00603-025-04937-3>
- Matasci B, Stock GM, Jaboyedoff M et al (2018) Assessing rockfall susceptibility in steep and overhanging slopes using three-dimensional analysis of failure mechanisms. *Landslides* 15:859–878
- Mavrouli O, Coroninas J (2018) Txt-tool 4.034-1.1: Quantitative rockfall risk assessment for roadways and railways. *Landslide Dynamics: ISDR-ICL Landslide Interactive Teaching Tools: Volume 2: Testing, Risk Management and Country Practices* pp 509–519
- McClung D (1999) The encounter probability for mountain slope hazards. *Can Geotech J* 36(6):1195–1196
- Melzner S, Rossi M, Guzzetti F (2020) Impact of mapping strategies on rockfall frequency-size distributions. *Eng Geol* 272:105639
- Mignelli C, Lo Russo S, Peila D (2012) Rockfall risk management assessment: the ro. ma. approach. *Natural hazards* 62(3):1109–1123
- Mineo S (2020) Comparing rockfall hazard and risk assessment procedures along roads for different planning purposes. *J Mt Sci* 17(3):653–669
- Moos C, Bontognali Z, Dorren L et al (2022) Estimating rockfall and block volume scenarios based on a straightforward rockfall frequency model. *Eng Geol* 309:106828
- Morgenstern NR (2018) Toward landslide risk assessment in practice. In: *Landslide risk assessment*. Routledge, p 15–23
- Muhlbauer WK (2004) Pipeline risk management manual: ideas, techniques, and resources. Elsevier
- Nama S, Maurya AK, Maji A et al (2016) Vehicle speed characteristics and alignment design consistency for mountainous roads. *Transportation in Developing Economies* 2:1–11
- Pandey VHR, Kushwaha G, Kainthola A et al (2025) Field data driven rockfall hazard and risk assessment along sangla-chitkul road, himachal pradesh, india. *Bull Eng Geol Env* 84(6):1–19
- Raibaut F, Ivanez O, Douthe C, et al (2025) Rockfalls trajectory: 3d models predictive capability assessment and coefficients calibration using optimization-based processes. *Engineering Geology* p 107937
- Rangavajhala S, Liang C, Mahadevan S (2012) Design optimization under aleatory and epistemic uncertainties. In: 12th AIAA Aviation Technology, Integration, and Operations (ATIO) Conference and 14th AIAA/ISSMO Multidisciplinary Analysis and Optimization Conference, p 5665
- Rwodzi L (2010) Rockfall risk: quantification of the consequences of rockfalls. PhD thesis
- UNI 11211-1 (2018) Opere di difesa dalla caduta massi - parte 1: Termini e definizioni
- UNI 11211-2 (2021) Opere di difesa dalla caduta massi - parte 2: Programma preliminare di intervento

- Scavia C, Barbero M, Castelli M et al (2020) Evaluating rockfall risk: some critical aspects. *Geosciences* 10(3):98
- Schmid SM, Fügenschuh B, Kissling E et al (2004) Tectonic map and overall architecture of the alpine orogen. *Eclogae Geol Helv* 97:93–117
- Shang K, Kossen Z (2013) Applying fuzzy logic to risk assessment and decision-making. *casualty actuarial society. Canadian institute of Actuaries, Society of Actuaries*–2013–59 p
- Shortridge J, Aven T, Guikema S (2017) Risk assessment under deep uncertainty: a methodological comparison. *Reliability Engineering & System Safety* 159:12–23
- Sim KB, Lee ML, Wong SY (2022) A review of landslide acceptable risk and tolerable risk. *Geoenvironmental Disasters* 9(1):3
- Straub D, Schubert M (2008) Modeling and managing uncertainties in rock-fall hazards. *Georisk* 2(1):1–15
- Strunden J, Ehlers TA, Brehm D et al (2015) Spatial and temporal variations in rockfall determined from tfs measurements in a deglaciated valley, switzerland. *J Geophys Res Earth Surf* 120(7):1251–1273
- Trappmann D, Corona C, Stoffel M (2013) Rolling stones and tree rings: a state of research on dendrogeomorphic reconstructions of rockfall. *Prog Phys Geogr* 37(5):701–716
- Turrin S, Hanss M, Selvadurai A (2009) An approach to uncertainty analysis of rockfall simulation. *Computer Modeling in Engineering & Sciences* 52(3):237–258
- Umili G, Taboni B, Ferrero AM (2023) Influence of uncertainties: a focus on block volume and shape assessment for rockfall analysis. *Journal of Rock Mechanics and Geotechnical Engineering* 15(9):2250–2263
- Volkwein A, Schellenberg K, Labiouse V et al (2011) Rockfall characterisation and structural protection-a review. *Nat Hazard* 11(9):2617–2651
- Wang X, Zhang L, Wang S et al (2012) Field investigation and rockfall hazard zonation at the shijing mountains sutra caves cultural heritage (china). *Environmental Earth Sciences* 66:1897–1908
- Wang X, Frattini P, Crosta G et al (2014) Uncertainty assessment in quantitative rockfall risk assessment. *Landslides* 11:711–722
- Wang X, Frattini P, Crosta G et al (2014) Uncertainty assessment in quantitative rockfall risk assessment. *Landslides* 11:711–722
- Wei LW, Chen H, Lee CF et al (2014) The mechanism of rockfall disaster: a case study from badouzh, keelung, in northern taiwan. *Eng Geol* 183:116–126
- Van Westen CJ, Castellanos E, Kuriakose SL (2008) Spatial data for landslide susceptibility, hazard, and vulnerability assessment: an overview. *Eng Geol* 102(3–4):112–131
- Zheng Y, Xie Y, Long X (2021) A comprehensive review of bayesian statistics in natural hazards engineering. *Nat Hazards* 108(1):63–91
- Zimmer VL, Sitar N (2015) Detection and location of rock falls using seismic and infrasound sensors. *Eng Geol* 193:49–60

Publisher's Note Springer Nature remains neutral with regard to jurisdictional claims in published maps and institutional affiliations.